Plant Science 233 (2015) 61–71

Contents lists available at ScienceDirect

Plant Science

journal homepage: www.elsevier.com/locate/plantsci

OsSEC24, a functional SEC24-like protein in rice, improves tolerance to iron deficiency and high pH by enhancing H^+ secretion mediated by PM-H^+-ATPase

Shuang Li[a], Xiao-Xi Pan[a], James O. Berry[b], Yi Wang[a], Naren[a], Shuang Ma[a], Song Tan[a], Wei Xiao[a], Wei-Zhong Zhao[c], Xian-Yong Sheng[a], Li-Ping Yin[a,*]

[a] College of Life Sciences, Capital Normal University, No. 105 Xisanhuan North Street, Beijing 100048, China
[b] Department of Biological Sciences, State University of New York, Buffalo, NY 14260, USA
[c] Institute of Mathematics and Interdisciplinary Sciences, Capital Normal University, No. 105 Xisanhuan North Street, Beijing 100048, China

ARTICLE INFO

Article history:
Received 9 September 2014
Received in revised form
29 December 2014
Accepted 1 January 2015
Available online 8 January 2015

Keywords:
Iron deficiency
OsSEC24
PM-H^+-ATPase
Tobacco
Rice
NMT

ABSTRACT

Iron is abundant in the soil, but its low solubility in neutral or alkaline soils limits its uptake. Plants can rely on rhizosphere acidification to increase iron solubility. OsSEC27p was previously found to be a highly up-regulated gene in iron-deficient rice roots. Here, pH-dependent complementation assays using yeast mutants *sec24Δ/SEC24* and *sec27Δ/SEC27* showed that OsSEC27 could functionally complement SEC24 but not SEC27 in yeast; thus, it was renamed as OsSEC24. We found that *OsSEC24*-transgenic tobacco plants increased the length and number of roots under iron deficiency at pH 8.0. To explore how OsSEC24 confers tolerance to iron deficiency, we utilized transgenic tobacco, rice and rice protoplasts. H^+ flux measurements using Non-invasive Micro-test Technology (NMT) indicated that the transgenic *OsSEC24* tobacco and rice enhanced H^+ efflux under iron deficiency. Conversely, the application of plasma membrane PM-H^+-ATPase inhibitor vanadate elucidated that H^+ secretion increased by OsSEC24 was mediated by PM-H^+-ATPase. OsPMA2 was used as a representative of iron deficiency-responsive PM-H^+-ATPases in rice root via RT-PCR analysis. In transgenic rice protoplasts OsPMA2 was packaged into OsSEC24 vesicles after export from the ER through confocal-microscopy observation. Together, OsSEC24 vesicles, along with PM-H^+-ATPases stimulate roots formation under iron deficiency by enhancing rhizosphere acidification.

1. Introduction

Iron is a plant nutrient that is essential for many cellular processes, including photosynthesis and respiration, etc. It is very abundant in soils, but exists predominantly as an insoluble ferric-hydroxide complex that is unavailable for root uptake in oxygenated soils at neutral or alkaline pH (normal aerobic soil conditions) [1]. Higher plants have developed two main strategies to solubilize and efficiently assimilate iron when this nutrient is limiting. Nongraminaceous monocot and dicot plants utilize an Fe-reduction strategy (Strategy I), whereas graminaceous monocots, including rice, typically make use of an Fe-chelation strategy (Strategy II) [2]. It is well known that Strategy II plants respond to iron deficiency by releasing phytosiderophores (PS), which solubilize inorganic Fe(III) complexes through chelation [1]. In rice, only deoxymugineic acid (DMA) is the primary PS released from roots to chelate Fe(III), forming Fe(III)-DMA complexes in soil. These are then transported into the roots by the Yellow Stripe (YS) transporter OsYSL15 that is specific for metal-PS chelation complexes. However, in rice the synthesis and diffusion of mugineic acid (MA) is limited under iron-deficient growth conditions, limiting its Strategy II uptake capability [3–5]. Therefore, while rice is considered to be a Strategy II plant, it also has an ability to solubilize and directly absorb iron from soil by means of Strategy I [3–6].

The Strategy I uptake system relies on acidification of soil within the rhizosphere to increase the solubility of ferric iron complexes at neutral or alkaline pH. The Fe(II) uptake occurs

Abbreviations: PS, phytosiderophores; MA, mugineic acid; YS, Yellow Stripe; FRO, Fe(III)-chelate reductase oxidase; PM, plasma membrane; COPII, Coat Protein II; COPI, Coat Protein I; ER, endoplasmic reticulum; GFP, green fluorescent protein; MS, Murashige and Skoog; SD, standard deviation; SE, standard error; EST, expressed sequence tag; TGN, trans Golgi network; CGN, cis-Golgi network; NMT, Non-invasive Micro-test Technology.

* Corresponding author. Tel.: +86 01068901692; fax: +86 01068901692.
E-mail address: yinlp@cnu.edu.cn (L.-P. Yin).

http://dx.doi.org/10.1016/j.plantsci.2015.01.001

through the activation of several enzymes at the root surface, most notably a P-type H^+-ATPase to release H^+ for acidification into the rhizosphere, an Fe(III)-chelate reductase oxidase (FRO2) to reduce Fe(III) to the more soluble Fe(II) form at the root surface, and a specific Fe(II) transporter (IRT1) for uptake of the soluble Fe(II) [1]. The H^+ extrusion mediated by PM H^+-ATPases in plant roots not only acidifies/solubilizes iron in the rhizosphere, but also powers the necessary transport processes by generating a pH gradient across the PM [7]. The H^+-ATPase associated with Strategy I iron uptake is a canonical plasma membrane (PM) protein that occurs in all organisms. In tomato, a Strategy I plant, H^+ export mediated by this enzyme causes a drop in the pH of the rhizophere, which enhances the expression of genes encoding FRO2 and the iron transporter IRT1 [8]. However, unlike typical Strategy I plants, *FRO* encoding mRNAs or FRO enzymatic activity are not present in Fe-deficient rice roots [5], indicating that uptake of Fe(II) occurs without the additional step of Fe(III) reduction. Thus, it appears that the Strategy I-like system in rice allows for the direct uptake of Fe(II), via the Fe(II) transporters OsIRT1 and OsIRT2 [5,6]. Taken together, evidence indicates that root H^+-ATPases serve as a central regulatory point to coordinate the activities and production of different components of the Strategy I uptake system, ensuring the efficient interactive functioning of this iron acquisition mechanism.

In addition to their role in iron assimilation from soil, PM H^+-ATPases are also implicated in the extensibility of plant cells. Based on the long-standing acid growth theory, auxin stimulates PM H^+-ATPases activity to pump H^+ into the apoplast, where the resulting decrease in apoplastic pH caused by increased H^+ excretion can activate cell wall-localized enzymes, such as expansin. Thus, it has been proposed that the activity of PM H^+-ATPases is essential for elongation growth of plant [9]. Furthermore, the recent studies provide molecular evidence for the acid growth theory. Auxin promotes phosphorylation of the C-terminal autoinhibitory domain of PM H^+-ATPases, by inhibiting the phosphatases activity of the PP2C-D protein at the PM. The proportion of active PM H^+-ATPases in the phosphorylated status increases, allowing for enhanced H^+ efflux, activation of cell wall-modifying enzymes and elongation of plant roots cells [10].

In summary, it appears that PM H^+-ATPases play a key role in regulating plant growth and development, being responsible for increasing iron uptake, and increasing extensibility growth of plant cells. This current study focuses on the iron responsiveness of PM-H^+-ATPase enzymes in rice roots. There are 10 gene family members that encode the rice PM H^+-ATPases (*OsPMA1* to *OsPMA10*), five of which, – *OsPMA1, OsPMA2, OsPMA3, OsPMA7* and *OsPMA8*, are known to be expressed in roots [11,12]. We show here that root-localized *OsPMA1, OsPMA2* and *OsPMA3* transcripts are upregulated under conditions of iron deficiency. We further demonstrate that the process of H^+ secretion, driven by PM-H^+-ATPase, is enhanced in iron-deficient rice roots, identifying this enzyme as a key determinant of the Strategy I system utilized by rice in response to iron deficiency.

PM proteins, including the PM-H^+-ATPase, are separated/sorted from other intracellular proteins at several points along the endoplasmic reticulum (ER) secretory pathway. Protein sorting is often mediated by small membrane vesicles that originate from the ER and travel to specific locations within the cell, mediated through Coat Protein I (COPI) and Coat Protein II (COPII) and clathrin coat [13]. Coat Protein II is associated with early stages of the secretory pathway, producing vesicles that move proteins from the ER to the cis-Golgi network (CGN) of Golgi apparatus. Coat Protein I is associated primarily with the backwards transport of vesicles from the CGN of Golgi to the ER. And clathrin coat mainly mediates large molecules endocytosis and secretory proteins exocytosis from the trans Golgi network (TGN) of Golgi apparatus [13–15].

In our previous study, a highly up-regulated gene in iron-deficient rice roots was identified through microarray analysis. The original EST fragment of a microarray displayed similarity to one component of COPI in yeast, SEC27, via the TBlastX search with the EST in yeast genome database (http://www.yeastgenome.org/cgi-bin/blast-sgd.); thus, it was initially referred to as *OsSEC27* (GenBank Accession No. ABE01836.1 at NCBI web; LOC_Os02g56500 at Rice Genome Annotation Project; 584 aa) [16]. The expression of *OsSEC27* in transgenic tobacco demonstrated the ability of this encoded protein to significantly enhance H^+ extrusion from roots hairs, relative to wild type control plants, under conditions of iron-deficiency [16]. Thereby, in order to characterize the authentic functions of OsSEC27 we performed functional complementation assays in yeast mutant strains, including *sec27Δ/SEC27*, *sec24Δ/SEC24*, *chc1Δ/CHC1*, *pma1Δ/PMA1* and *aft1Δ/AFT1* that are defective in formation of coat protein complexes COPI [15], COPII [17], clathrin coat protein [14], PM-H^+-ATPase PMA1 [18] and iron-deficiency regulated transcription factor AFT1 [19]. Based on the ability of this protein to functionally complement SEC24, but not SEC27, PMA1, CHC1 or AFT1 in yeast, we have renamed this protein as OsSEC24, a functional Sec24-like protein. This current study extends our characterization of OsSEC24 by exploring how this vesicular protein, together with PM-H^+-ATPase, enhanced H^+ extrusion in rice roots and affected plant growth under conditions of iron deficiency and high pH levels.

2. Materials and methods

2.1. Yeast strains, culture medium and plasmids construction

The yeast strains presented in this paper were as follows: BY4743 [wild type] (*MAT*a/*MAT*α; *his3Δ1/his3Δ1; leu2Δ0/leu2Δ0; met15Δ0/MET15; LYS2/lys2Δ0; ura3Δ0/ura3Δ0*), BY4743 *sec24Δ/SEC24* (BY4743 with *YIL109c::kan^R/YIL109c*). BY4743 *sec27Δ/SEC27* (BY4743 with *YGL137w::kan^R/YGL137w*). Yeast transformants were selected on the synthetic defined (0.67% yeast nitrogen base without amino acids) medium supplemented with 2% galactose and any necessary auxotrophic requirements (-Uracil) (SD medium). And the nontransformed yeast cells were grown on SD medium supplemented with 20 μg/ml Uracil (SC medium). Yeast cell cultures were diluted to an optical density of 0.1, 0.01, 0.001, 0.0001. Then 3 μl of each cell suspension was spotted on SD and SC media at different pH levels (pH 4.0, 6.0, 8.0, 8.5, 9.0), respectively. The plates at pH 6.0 were incubated at 28 °C and 37 °C. The translated region of *OsSEC24* and *OsPMA2* was cloned into the galactose-inducible vector pYES2.0(P_{GAL1})-*Ura* with *GFP and mCherry*, respectively. Promoter(P_{GAL1})-*OsSEC24-GFP*-Terminator from pYES2.0-*Ura* was cloned into the YEplac181-*Leu* vector. The coding region of *OsSEC24-GFP* and *OsPMA2-mCherry* was separately cloned into pBI221 vector and pBIN20 vector, respectively, under the control of the 35S promoter. The primers used for cloning were listed in Table S1.

2.2. Protoplast isolation and transient expression

Protoplasts isolation from rice suspension cells and transient expression were performed as follows [20–22]. After 5 days of culturing, rice suspension cells were harvested and incubated in an enzyme solution (0.6 M mannitol, 10 mM MES, pH 5.7, 1.5% cellulase RS, 0.75% macerozyme, 1 mM $CaCl_2$ and 0.1% bovine serum albumin) for 1 h at 26 °C with gentle agitation (50–75 rpm). The protoplasts were isolated from the undigested material with a cell strainer and centrifuged at 2000 rpm, 4 °C for 15 min. They were then resuspended in 5 mL of W5 solution (154 mM NaCl, 5 mM KCl, 125 mM $CaCl_2$ and 2 mM MES, pH 5.7) and pelleted

again by centrifugation for 15 min at 2000 rpm, 4 °C. These pelleted protoplasts were resuspended in MMG solution (15 mM $MgCl_2$, 0.6 M mannitol and 4 mM MES, pH 5.7) at room temperature. And then, the protoplasts were mixed with plasmid and incubated in PEG3350/Ca solution (40% PEG3350, 0.6 M mannitol, 0.1 M $CaCl_2$) for 15 min in the dark for transformation. The transgenic protoplasts were washed with W5 and centrifuged at 2000 rpm for 15 min. Finally, the protoplasts were resuspended gently with 1 mL incubation solution (0.6 M mannitol, 4 mM KCl, 154 mM NaCl, 125 mM $CaCl_2$, 4 mM MES, pH 5.8) in a plate, and incubated at room temperature for 20–25 h.

2.3. The transformation of rice and tobacco plants and vanadate treatment

pCAMBIA1302-*OsSEC24-GFP* was transformed into tobacco plants (*Nicotiana tabacum* var. *Samsun NN*) or rice plant (*Oryza sativa L. cv. Japonica*) using *Agrobacterium* EHA105 mediated transformation. The detailed methods were described previously [21,23]. The T3 transgenic tobacco plants and T1 transgenic rice plants were used in subsequent research. The plants seedling roots were cultured in −Fe and +Fe, then exposed to testing solution with 500 μM Na_3VO_4 (13721-39-6, Sigma) for 10 min and were prepared for H^+ flux measurement.

2.4. H^+ flux measurement

The net H^+ flux was measured using Non-invasive Micro-test Technology (NMT) (Xuyue (Beijing) Sci. & Tech. Co. Ltd.) (BeiJing, China; http://www.xuyue.net). H^+ ion-selective microelectrodes with an external tip diameter of c. 3 μm were manufactured. Only electrodes with Nernstian slopes > 56 mV per decade were used. The samples were measured in the testing solution at pH 5.8 after electrodes were calibrated at 2 pH levels (solution I, pH 5.5 and solution II, pH 6.0). Proton fluxes were calculated by MageFlux (~~Younger USA Corp.~~ http://youngerusa.com/mageflux) which is based on Fick's law of diffusion. The detailed methods were described previously [16].

2.5. pH measurement

The transgenic tobacco and wild type grown on Murashige and Skoog (MS) solid medium at pH 5.8 for one week were transferred to MS liquid medium at pH 5.8 for one week under −Fe and +Fe (100 μM) conditions, respectively. The pH value was determined after one week of the two iron regimes treatment. The experiment was repeated three times, and the pH in MS culture solution was adjusted to pH 5.8 for each time. The transgenic yeast cells were cultured in the growth medium containing glucose and then transferred to the galactose-containing medium for 24 h at pH 5.8. The pH value was measured and the experiment was repeated three times.

2.6. Confocal microscopy

The cells were washed with PBS and viewed by confocal microscopy (LSM 5 Live, Zeiss, Germany). Excitation/emission parameters for GFP, ER-tracker Blue White and mCherry were 488 nm/520–555 nm, 405 nm/415–480 nm, 561 nm/575 nm, respectively. All images were recorded and analyzed with Zeiss Zen 2007 software.

2.7. Semi-quantitative RT-PCR analysis

3-Week-old rice plants grown on MS were exposed to −Fe and +Fe (100 μM) conditions, respectively, for one week. Total RNA from rice roots was isolated using an RNAprep Pure Plant Kit (Beijing Tiangen Biotech Co., Ltd., China) according to the manufacture's protocol. First-strand cDNA was synthesized from total RNA (1 μl) by reverse transcription using oligo (dT) primers and reverse transcriptase (QuantScript RT Kit; Beijing Tiangen Biotech Co., Ltd., China). The PCR was performed, using *OsPMA1–OsPMA10* genes-specific primers. The primers were listed in Table S1.

3. Results

3.1. A highly upregulated gene in iron-deficient rice roots is initially named OsSEC27

A microarray assay of 10532 cDNAs derived from rice expressed sequence tag (EST) revealed gene expression profiles in rice roots after 5 days of Fe-deficiency in our previous study [24]. Fold Change (FC) was widely utilized as a method for analyzing differentially expressed genes in microarray data [25]. Levels of change, (e.g. 0.5 for down and 2 for up-regulated) were applied to screen the genes under or above thresholds [25]. In our previous microarray datasets, 203 clones were classified as upregulated genes upon Fe-deficiency via two-color ratio (Cy5/Cy3) analysis, containing a transcript of high −Fe/+Fe (+Fe is 100 μM EDTA-Fe^{2+} for short) ratio at 8.205 [24,26]. (Fig. S1A). The highly up-regulated gene cloned from Fe-deficient rice roots was 99% identical to the original EST fragment; thus, the gene encoding protein can be used for the following functionality identification (Fig. S1B). PSI-Blast search at the NCBI website showed that the encoded protein (LOC_Os02g56500 identified by Rice Genome Annotation Project) shared a high identity and similarity to 3 proteins from Strategy I-type *Arabidopsis thaliana* and 2 proteins from Strategy I-type *Solanum lycopersicum* in their amino acid sequence. Unfortunately, the functions of those proteins remain uncharacterized. In Strategy II-type *Hordeum vulgare* or *Zea mays, Saccharomyces cerevisiae* and *Homo sapiens*, we did not find proteins which had homology with Os02g56500 protein in rice (Fig. S1C). However, the original EST fragment used in the microarray assay displayed a little bit of similarity to one component of COPI in yeast, SEC27, via the TBlastX search with the EST nucleotide sequence in yeast genome database (http://www.yeastgenome.org/cgi-bin/blast-sgd) (Fig. S1D); thus, this up-regulated gene upon iron deficiency was initially referred to as *OsSEC27* [16].

3.2. OsSEC27 is renamed OsSEC24 because the Os02g56500 protein functionally complements SEC24 in yeast

Yeast cells provide an excellent model system in which the role of functionally conserved exogenous proteins can be determined by complementation [22,27–30]. In order to characterize the authentic functions of OsSEC27, we first expressed a cDNA encoding the heterologous rice protein OsSEC27 in the mutant yeast strains including *sec27Δ/SEC27*, *sec24Δ/SEC24*, *chc1Δ/CHC1*, *pma1Δ/PMA1* and *aft1Δ/AFT1* that are defective in formation of coat protein complexes COPI [15], COPII [17], clathrin coat protein [14], PM-H^+-ATPase PMA1 [18] and iron-deficiency regulated transcription factor AFT1 [19]. Due to the lack of complementation of OsSEC27 in *chc1Δ/CHC1*, *pma1Δ/PMA1* and *aft1Δ/AFT1* yeast strains (data not shown), we chose *sec27Δ/SEC27*, *sec24Δ/SEC24* yeast strains for functional analysis of OsSEC27. The wild type (WT), *sec27Δ/SEC27*, *sec24Δ/SEC24* strains presented in this study are all defective in uracil (Ura) synthesis, and the two *sec* mutant strains are considered to be temperature sensitive [15,31]. Therefore, we first characterized the growth of these strains on different media (synthetic defined media with and without uracil supplement, designated SC media and SD media, respectively) and at different

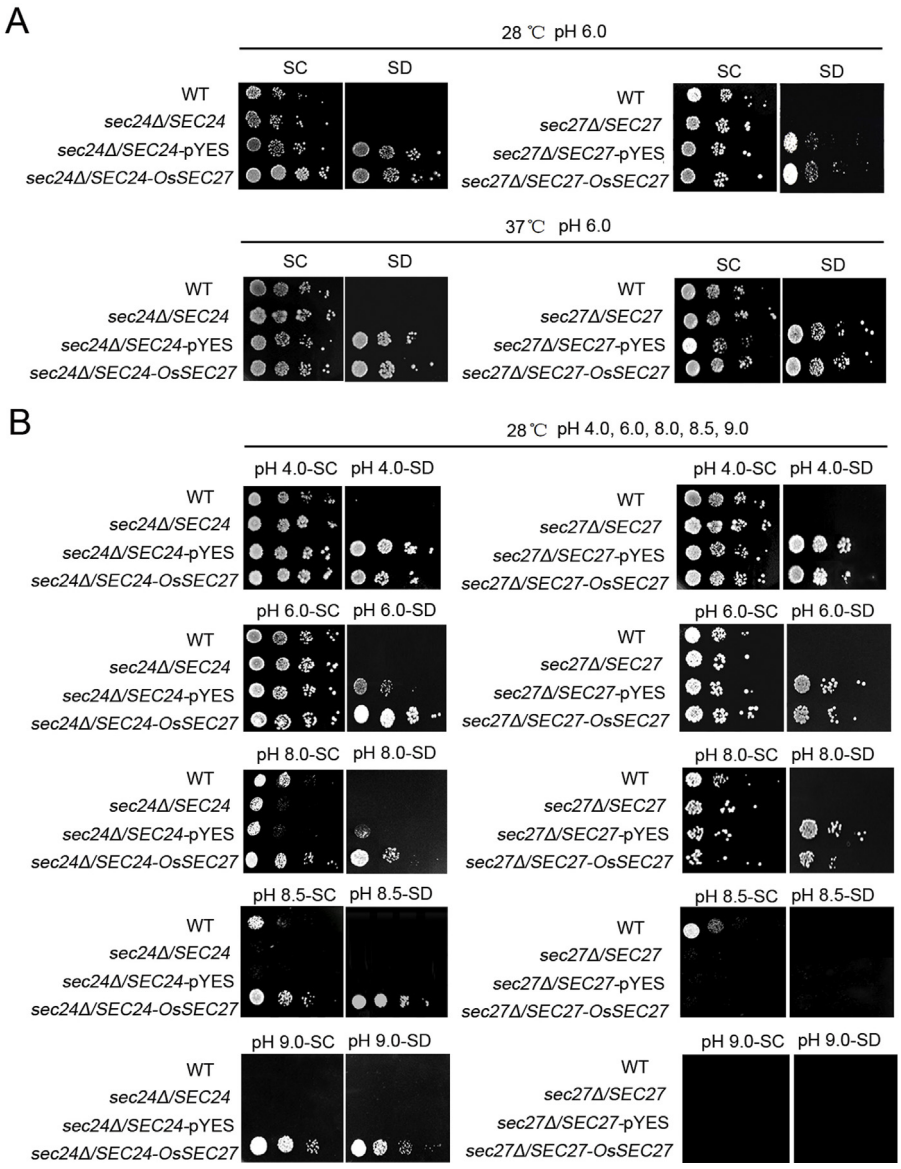

Fig. 1. Functional complementation of OsSEC27 in *sec24Δ/SEC24* and *sec27Δ/SEC27* yeast strains. (A) The temperature-sensitive test of *sec27Δ/SEC27* and *sec24Δ/SEC24* yeast strains. The wild type (WT), *sec24Δ/SEC24*, pYES vector-transgenic *sec24Δ/SEC24*, and *OsSEC27*-transgenic *sec24Δ/SEC24* (left) and WT, *sec27Δ/SEC27*, pYES vector-transgenic *sec27Δ/SEC27*, and *OsSEC27*-transgenic *sec27Δ/SEC27* (right) cells were grown on a synthetic defined medium without uracil (SD-Ura medium) containing galactose or on the same medium supplemented with Ura (SC medium) at 28 °C and 37 °C, respectively. (B) The pH-sensitive test of *sec27Δ/SEC27* and *sec24Δ/SEC24* yeast strains and functional complementation of OsSEC27. The yeast strains indicated in (A) were grown on a synthetic defined medium without uracil (SD-Ura medium) containing galactose or on the same medium supplemented with Uracil (SC medium) at various pH levels (pH 4.0, pH 6.0, pH 8.0, pH 8.5, and pH 9.0) at 28 °C. Yeast cultures were diluted to optical density of 0.1, 0.01, 0.001, and 0.0001.

temperatures (i.e. permissive 28 °C and nonpermissive 37 °C), using a serial dilution drop test. As expected, the growth of all three yeast strains was supported on medium supplemented with Uracil (Fig. 1A, 28 °C, SC), while medium lacking the uracil supplement (Fig. 1A, 28 °C, SD) did not support the growth of these strains. However, the growth phenotypes of the *sec27Δ/SEC27*, *sec24Δ/SEC24* mutant strains showed the same trait both at 37 °C and 28 °C (Fig. 1A, 37 °C and 28 °C, SC), and so the mutants were not influenced by temperature. Transformation of these strains with a pYES-*Ura* vector alone (control) and the pYES-*Ura*-*OsSec27* construct rescued the Ura-limited growth defects of the *sec27Δ/SEC27*, *sec24Δ/SEC24* yeast strains, respectively, at both temperatures (Fig. 1A, 28 °C and 37 °C, SD). The observation of identical growth characteristics for the wild type, mutant, and transformant yeast cells at 28 °C and 37 °C demonstrated that both *sec* mutants were suitable for use as experimental host strains for complementation analysis with a pYES-*Ura* yeast transformation vector, and that temperature was not a determining factor for their growth characteristics. Next, for the pH-dependent studies described below, all of the yeast strains were grown at 28 °C.

During the pH-sensitive test of *sec27Δ/SEC27* and *sec24Δ/SEC24* strains, we found that the growth of *sec27Δ/SEC27*, *sec24Δ/SEC24* and the vector transformant cells was gradually impaired when the external pH was increased from pH 4.0 to 8.5, and even was completely stopped at pH 9.0 (Fig. 1B). In contrast, *OsSEC27*-transgenic *sec24Δ/SEC24* displayed better growth performance from pH 4.0 to pH 9.0 (Fig. 1B, left). The heterologous OsSEC27 reversed the pH-sensitive growth defect of the *sec24Δ/SEC24* strain, suggesting that SEC24 of COPII in yeast plays an important role in cell viability at high pH, and that OsSEC27 is able to functionally complement SEC24 in yeast. Further confirmation for this conclusion came from the negative complementation of OsSEC27 in *sec27Δ/SEC27*.

Obviously, the growth of *OsSEC27*-transgenic *sec27Δ/SEC27* was inhibited at pH 8.5 relative to *OsSEC27*-transgenic *sec24Δ/SEC24* (Fig. 1B, right). Intriguingly, SEC24 in vivo did not support the growth of wild type at pH 9.0 compared with *OsSEC27*-transgenic *sec24Δ/SEC24*; this result indicated that exogenous OsSEC27 conferred more tolerance to high pH levels than did endogenous SEC24 in yeast (Fig. 1B, pH 9.0). Given that OsSEC27 could functionally replace SEC24 but not SEC27 in yeast, the protein was designated as OsSEC24.

3.3. Transgenic OsSEC24 yeast enhances H^+ secretion at high pH

To assess the role of OsSEC24 in tolerance of high pH, we analyzed the real-time kinetics of the H^+ flux in the *sec24Δ/SEC24*, *GFP*- or *OsSEC24-GFP*-transgenic *sec24Δ/SEC24* at pH 6.0 and *OsSEC24-GFP*-transgenic *sec24Δ/SEC24* at pH 9.0, using a non-invasive H^+-selective microelectrode of NMT. Notably, the H^+ flux in both cases exhibited a two-phase response, with both influx and efflux oscillation patterns. At pH 6.0, compared to *sec24Δ/SEC24* and *GFP* transformants, *OsSEC24-GFP* transformants displayed attenuated H^+ influx and enhanced H^+ efflux (Fig. 2A). The mean rate of H^+ efflux in the *OsSEC24-GFP* transformants was markedly higher than that in *GFP* transformants (Fig. 2B). There was no significant difference in H^+ flux between *sec24Δ/SEC24* and *GFP* transformants ($p > 0.05$, Student's *t*-test; Fig. 2B). Furthermore, at pH 9.0, the kinetics and mean rate of H^+ flux showed that *OsSEC24-GFP* transformants exhibited stronger H^+ efflux than those at pH 6.0 (Fig. 2A and B). Thus, *OsSEC24*-transgenic *sec24Δ/SEC24* at high pH increased H^+ secretion. These results can explain why *OsSEC24* transformation improved *sec24Δ/SEC24* strain's tolerance to high pH in the assays of functional complementation in yeast (Fig. 1B).

3.4. Transgenic OsSEC24 tobacco increases the number and length of roots under iron deficiency and high pH

Given that the root phenotype is typical of iron-deficient plants [32], we decided to continue testing whether OsSEC24 plays a role in plant root growth under iron deficiency (−Fe). Aside from −Fe conditions [32], high pH can also stimulate H^+ secretion as shown in Fig. 2; thus, we cultivated transgenic tobacco that constitutively expresses *OsSEC24* at three pH levels (pH 4.0, pH 6.0 and pH 8.0), along with the wild type at pH 8.0, each pH under two iron regimens (−Fe, +Fe). The length of roots in the transformed tobacco was found to markedly increase from pH 4.0 to 8.0, irrespective of iron status, the effect being more pronounced under the high pH condition (pH 8.0; Fig. 3A, pH 4.0–8.0). Nevertheless, morphological comparison of the wild type and transgenic tobacco showed that the wild type tobacco, in general, displayed inhibition of root growth at pH 8.0 (Fig. 3A, pH 8.0). We also measured the length of tobacco roots in six 4-week-old seedlings both under −Fe and +Fe at each pH level. Consistent with the phenotypic differences, biostatistic assays revealed that the average root length of transgenic tobacco in sextuplicate

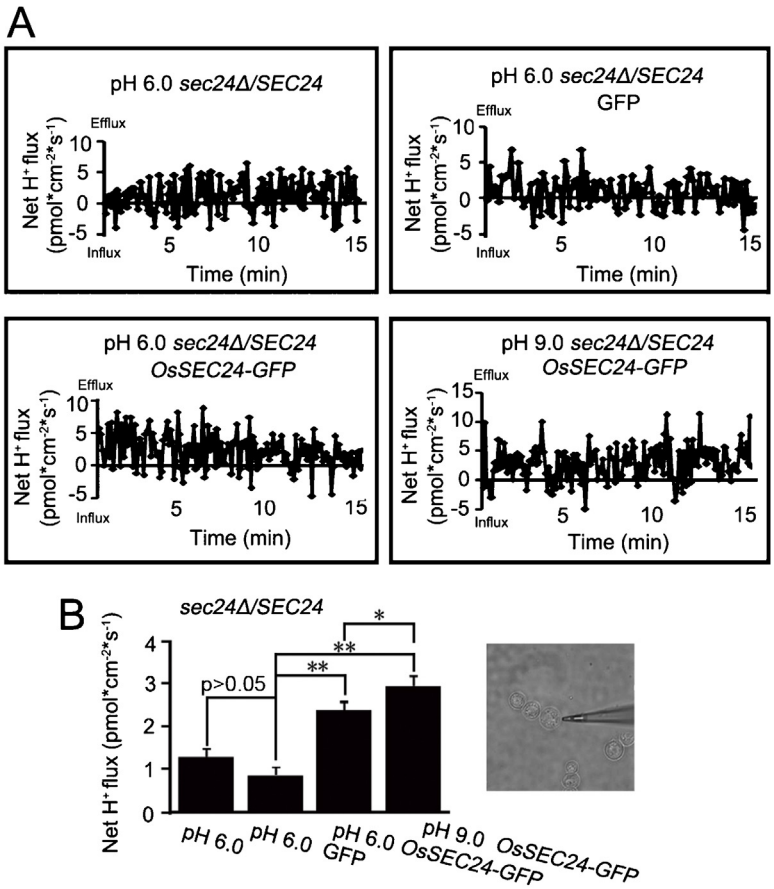

Fig. 2. The effect of OsSEC24 on net H^+ flux in transgenic yeast at high pH by NMT. (A) Kinetics of H^+ flux in *sec24Δ/SEC24*, *GFP*-transgenic *sec24Δ/SEC24*, and *OsSEC24-GFP*-transgenic *sec24Δ/SEC24* yeast cells at pH 6.0 and *OsSEC24-GFP*-transgenic *sec24Δ/SEC24* yeast cells at pH 9.0. The experiment was performed three times. Results from a representative experiment are shown. (B, left) The mean rates of H^+ flux in (A), using the mean value of three independent measurements (mean ± SE; $n = 3$). Every independent measurement contained >150 replicates. The image shows the measuring position using H^+-selective microelectrode of NMT (B, right). *Significant difference, $p < 0.05$ in Student's *t*-test; **extreme significant difference, $p < 0.01$ in Student's *t*-test.

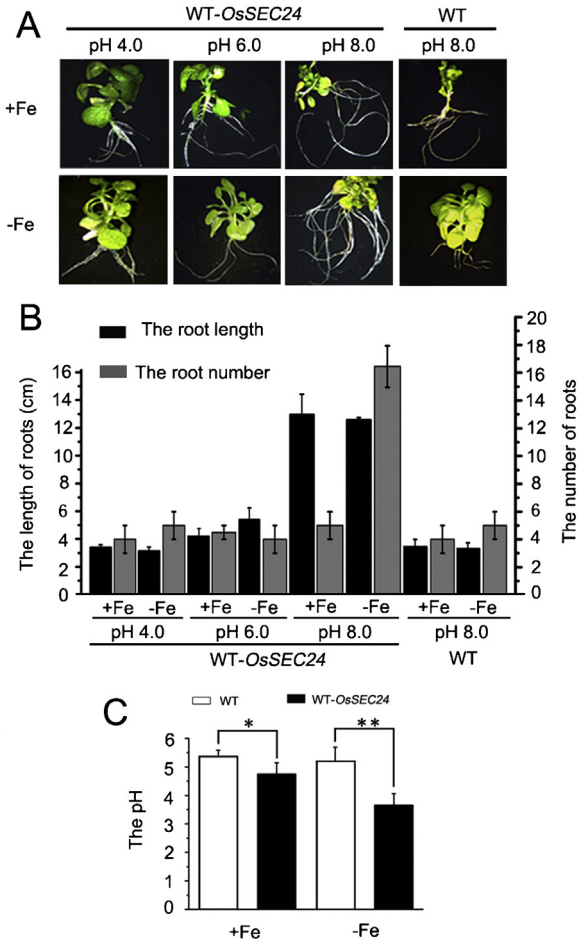

Fig. 3. Growth performance of wild type and *OsSEC24*-transgenic tobacco roots under different Fe and pH conditions. (A) The root phenotype of wild type (WT) and *OsSEC24*-transgenic tobacco seedlings grown in the culture solution supplied with 100 μM (+Fe) or no iron (−Fe) for four weeks at various pH levels (pH 4.0, pH 6.0, and pH 8.0). (B) The root length and number of WT and *OsSEC24*-transgenic tobacco seedlings in (A). The bars represent the average of root length and root number from 6 seedlings under −Fe and +Fe separately at each pH level ± SD ($n = 6$). For each replicate, all the roots were measured to calculate the mean root length. (C) The pH in the culture solution of WT and *OsSEC24*-transgenic tobacco seedlings after one week of −Fe and +Fe at pH 5.8. Data represent mean ± SD ($n = 5$). $^{*}p < 0.05$ in Student's *t*-test; $^{**}p < 0.01$ in Student's *t*-test.

at pH 8.0 was much greater than that of the transgenic plants at other pH levels and the wild type at pH 8.0 (Fig. 3B, pH 4.0–8.0). Intriguingly, the growing transgenic *OsSEC24* tobacco under −Fe at pH 8.0 showed a significant increase in the number of roots compared to the transgenic plants grown under +Fe and the wild type (Fig. 3A and B, pH 8.0). In contrast to the wild type, a clear increase in root number and length of transgenic *OsSEC24* tobacco under −Fe at pH 8.0 suggested that OsSEC24 conferred tolerance to −Fe at high pH levels by inducing root formation.

To determine the reason why OsSEC24 made transgenic *OsSEC24* tobacco more tolerant of −Fe relative to the wild type, we grew the transgenic *OsSEC24* tobacco seedlings and the wild type under −Fe and +Fe at pH 5.8, respectively. After measuring pH of the culture solution, we found that the mean pH ± SD ($n = 5$) for transgenic tobacco decreased compared to the wild type plants, the attenuated trend being more obvious under −Fe (Fig. 3C). Together, the data of pH measurement under −Fe, along with the phenotype of *OsSEC24*-transgenic tobacco roots under −Fe at pH 8.0, was consistent with the acid growth theory [9,10]. And OsSec24 improved tobacco tolerance to −Fe by enhancing the acidification of rhizospheres.

3.5. H^+ secretion increased by OsSEC24 is attributable to PM H^+-ATPase in tobacco and rice

Further support for the above-mentioned conclusion came from measurements of H^+ flux using a vibrating probe. As the real-time kinetics and the mean rate of H^+ flux showed that under −Fe, the transgenic tobacco root hairs exhibited significantly higher H^+ efflux rates than those under +Fe and wild type control (Fig. 4A and B). This result suggested that OsSEC24 enhanced H^+ secretion, particularly under −Fe, further explaining why *OsSEC24*-transgenic tobacco plants were more tolerant of −Fe than wild type (Fig. 3A, pH 8.0, −Fe). Acidification of the apoplast and rhizosphere by H^+ extrusion was demonstrated to correlate with the increase in the PM H^+-ATPase activity [33]. To confirm whether the H^+ extrusion enhanced by OsSEC24 was related to PM H^+-ATPase, one pharmacological agent, vanadate, an inhibitor of plant cell PM H^+-ATPase [34], was applied to the roots of the transgenic and wild type tobacco after −Fe and +Fe treatment, respectively (Fig. 4A and B, vanadate). The measurement of H^+ flux rates showed that the tobacco roots displayed a significantly weaker H^+ efflux in the presence of vanadate than without vanadate treatment.

Further evidence consistent with that finding came from H^+ flux measurements in transgenic rice plants expressing *OsSEC24* and wild type rice plants cultured in −Fe and +Fe conditions, respectively, in the presence or absence of vanadate. The real-time kinetics of H^+ flux showed that both wild type and transgenic rice roots exhibited continuous H^+ efflux under −Fe and +Fe, respectively (Fig. 5A). Nevertheless, the magnitude of the H^+ efflux in transgenic rice under −Fe was almost 1-fold higher than that under +Fe and >2-fold higher than that in the wild type (Fig. 5B). However, the exposure of both transgenic plants and the wild type to vanadate attenuated the H^+ efflux in the root hairs to a similar level, regardless of iron supply (Fig. 5A and B, vanadate); this result was consistent with the H^+ flux measurements in transgenic-tobacco root hairs. Therefore, the experiments with vanadate in both tobacco and rice showed that H^+ secretion promoted by OsSEC24 under −Fe is attributable to PM H^+-ATPase.

3.6. *OsPMA2 represents an iron deficiency-responsive PM-H^+-ATPase in rice root*

To determine how OsSEC24, together with PM H^+-ATPase in rice promotes H^+ extrusion, we first identified the −Fe-responsive PM H^+-ATPase isogenes in rice roots. After multiple sequence alignments of OsPMA-family proteins, phylogenetic analysis indicated that OsPMA1, OsPMA2, and OsPMA3 most likely shared a similar function (Fig. 6A, bottom). PCR analysis with gene-specific primers showed that four out of the 10 P-type H^+-ATPase isogenes (*OsPMA1* to *OsPMA10*) were expressed in roots (Fig. 6B). After imposing −Fe and +Fe for 3 d, semi-quantitative RT-PCR analysis of H^+-ATPase transcripts from rice roots showed that the *OsPMA1* and *OsPMA2* genes displayed a much higher transcriptional level under −Fe than under +Fe (Fig. 6C). The *OsPMA3* transcript was found to be slightly upregulated, whereas the *OsPMA7* gene, one of the major H^+-ATPase isoforms expressed in roots, was not transcriptionally regulated by −Fe (Fig. 6C). Based on the transcription level, *OsPMA1*, *OsPMA2*, and *OsPMA3* are the −Fe-responsive isogenes in roots. And we chose *OsPMA2* as a representative of iron deficiency-responsive PM-H^+-ATPases in rice root for the following experiments.

3.7. *The PM sorting of OsPMA2 depends on SEC24*

To clarify the role of OsSEC24 in PM sorting of OsPMA2, we grew transgenic yeast. In the transgenic *OsPMA2-mCherry* wild type, the majority of OsPMA2 was present at the PM; in contrast, in *OsPMA2-mCherry*-transgenic *sec24Δ/SEC24* strain, OsPMA2 was dispersed

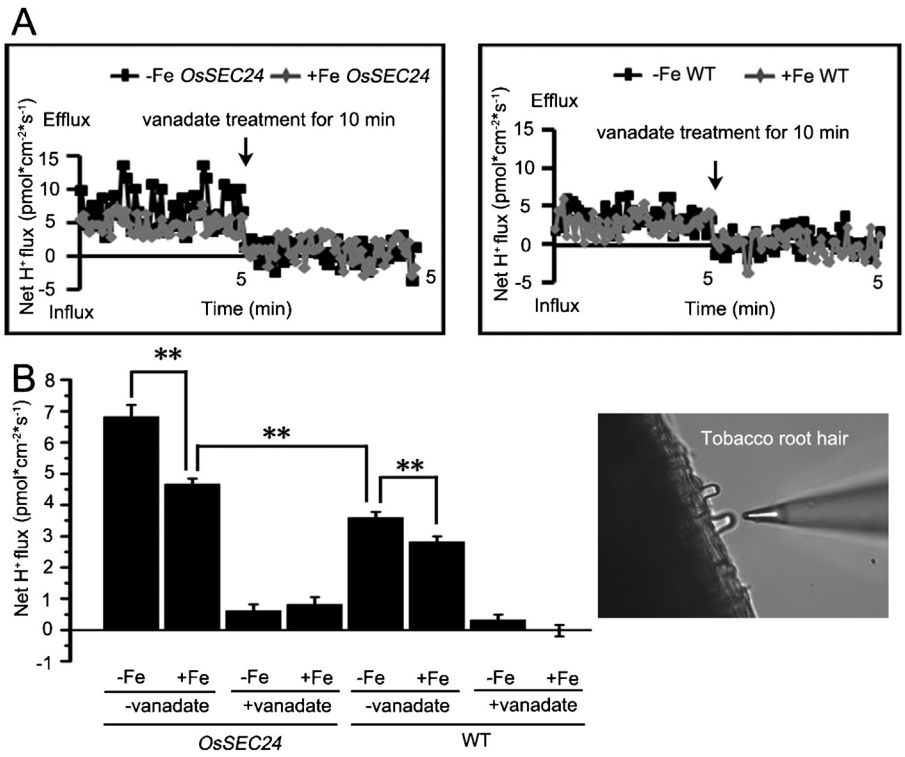

Fig. 4. The effects of OsSEC24 on H^+ extrusion in transgenic tobacco roots under −Fe and vanadate. (A) Kinetics of H^+ flux rates in WT and *OsSEC24*-transgenic tobacco seedlings grown on a −Fe or +Fe medium for 10 days and transferred to a culture solution containing vanadate (incubation for 10 min). (B, left) the mean rates of H^+ flux in (A), using the mean value of four independent measurements (mean ± SE). Two roots in each plant and two root hairs in each root were measured. Every independent measurement contained >50 replicates. The image shows the measuring position using H^+-selective microelectrode of NMT (B, right). $^{**}p < 0.01$ in Student's *t*-test.

within the cytoplasm with no specific signal found near the PM. These findings indicated that SEC24 coat protein plays an important role in PM sorting of OsPMA2 (Fig. 7A, top). However, *OsSEC24* introduction restored the defect in the PM targeting of OsPMA2 in the *sec24Δ/SEC24* strain (Fig. 7A, bottom). Eventually, OsSEC24 exhibited a dispersive pattern in the cytoplasm (Fig. 7A, bottom). Therefore, OsSEC24 functionally compensates for SEC24 in yeast for PM sorting of OsPMA2.

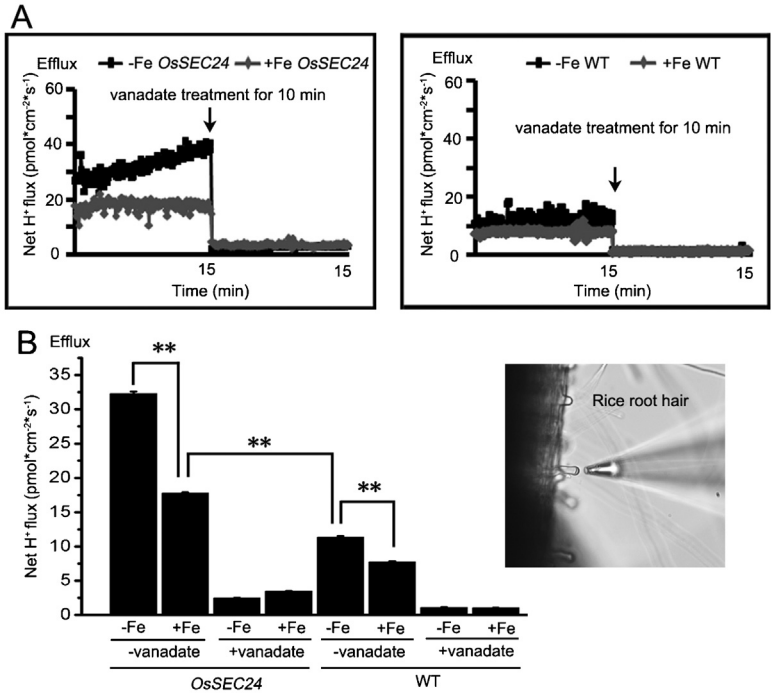

Fig. 5. The effects of OsSEC24 on H^+ extrusion in transgenic rice roots under −Fe and vanadate. (A) Kinetics of H^+ flux in WT and *OsSEC24* transgenic rice roots grown on −Fe or +Fe medium for two weeks and transferred to a culture solution containing vanadate (incubation for 10 min). (B, left) The mean rates of H^+ flux in (A), using the mean value of four independent measurements (mean ± SE). Two roots in each plant and two root hairs in each root were assayed. Every independent measurement contained >150 replicates. The image shows the measuring position using H^+-selective microelectrode of NMT (B, right). $^{**}p < 0.01$ in Student's *t*-test.

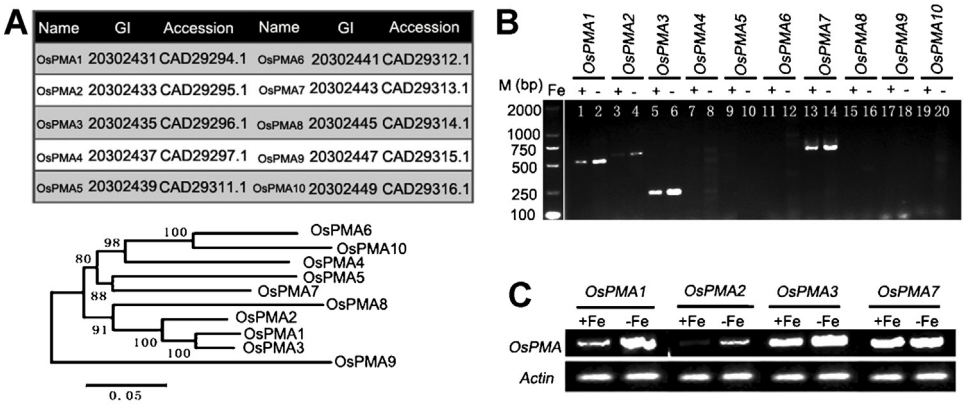

Fig. 6. Quantification of mRNA in OsPMA isoforms from rice roots under −Fe. (A) The GenBank database accession numbers for OsPMA1 to OsPMA10 (top). A dendrogram showing amino acid sequence similarities among the OsPMA family members in rice (bottom). The tree was constructed using all sequences shown in (A). The phylogenetic analysis was performed using protein sequences aligned in ClustalW. The tree was constructed using the Neighbor-Joining algorithm, with the following parameters: pairwise deletion, Poisson correction, and 1000 replicates for estimation of the bootstrap confidence level. (B) The expression analysis of OsPMA-family isogenes at the transcriptional level in roots by PCR under −Fe and +Fe, respectively. M: Marker. (C) Semiquantitative RT-PCR analysis of *OsPMA1*, *OsPMA2*, *OsPMA3*, and *OsPMA7* transcripts in rice roots under −Fe and +Fe. β-Actin expression is shown as a loading control.

The localization study using confocal microscopy is only a qualitative assessment of the OsSEC24 function. Consequently, H^+ flux measurements were carried out in the transgenic wild type yeast to quantify OsSEC24's importance in this transport pathway. By measuring real-time kinetics of H^+ flux, we found that the double *OsPMA2-mCherry*- and *OsSEC24-GFP* transformants exhibited a significant increase in efflux rates compared to the single *OsPMA2-mCherry* transformants, *mCherry* plus *GFP* double vectors-transformants and wild type (Fig. 7B). The mean rate of H^+ flux in the transformants expressing both *OsPMA2-mCherry* and *OsSEC24-GFP* was 1-fold higher than that in only *OsPMA2-mCherry* transformants and almost 9-fold higher than that in the *mCherry* plus *GFP* double vectors transformants and wild type, respectively (Fig. 7C). Moreover, after 24 h of culture at pH 5.8,

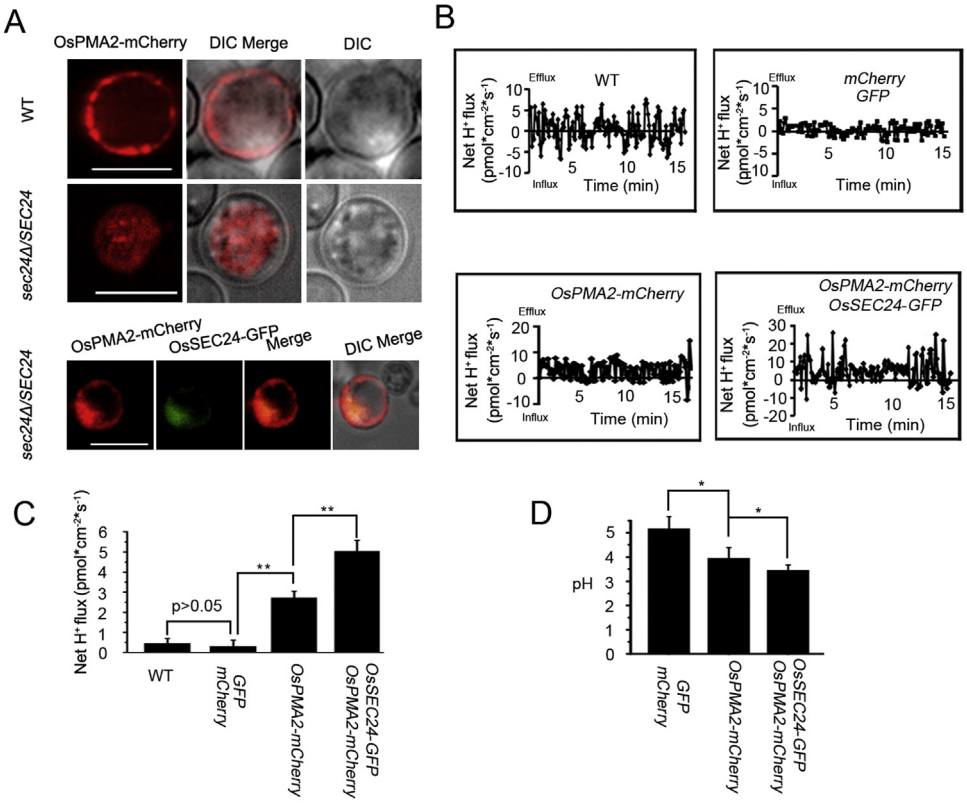

Fig. 7. The role of OsSEC24 in the PM sorting of OsPMA2 in yeast. (A) The localization observation of OsPMA2 in *OsPMA2-mCherry* single transgenic wild type (WT), *OsPMA2-mCherry* single transgenic *sec24Δ/SEC24*, and *OsPMA2-mCherry* plus *OsSEC24-GFP* double-transgenic *sec24Δ/SEC24* yeast cells. The scale bars for the panel are 5 μm. DIC, Differential Interference Contrast. (B) Kinetics of H^+ flux in WT, *mCherry* plus *GFP* double-transformants, *OsPMA2-mCherry* single-transformants and *OsPMA2-mCherry* plus *OsSEC24-GFP* double-transformants, respectively. The experiment was performed three times. Results from a representative experiment are shown. (C) The mean rates of H^+ flux in (B), using the mean value of three independent measurements (mean ± SE; $n = 3$). Every independent measurement contained >150 replicates. $^{**}p < 0.01$ in Student's *t*-test. (D) The pH in the culture solution of *mCherry* and *GFP* double-transgenic WT, *OsPMA2-mCherry* transgenic WT as well as *OsPMA2-mCherry* plus *OsSEC24-GFP* double-transgenic WT respectively, after 24 h of culture at pH 5.8. Data represent mean ± SD ($n = 3$). $^{*}p < 0.05$ in Student's *t*-test.

the pH level in the culture medium with the double *OsPMA2-mCherry*- and *OsSEC24-GFP* transformants decreased significantly relative to *OsPMA2-mCherry* transformants or *mCherry* plus *GFP* double transformants (Fig. 7D). This result was consistent with the H^+ flux measurements. Taken together, SEC24 coat protein is a key contributor to the PM sorting of OsPMA2; OsSEC24 rescues the loss of SEC24 in *sec24Δ/SEC24*; while exogenous OsSEC24 has stronger capacity for H^+ secretion than does endogenous SEC24 in yeast, which can explain why the growth of *OsSEC24* transgenic *sec24Δ/SEC24* was supported at pH 9.0 in contrast to wild type in Fig. 1B.

3.8. *OsSEC24 expression in rice increases the H^+ secretion mediated by OsPMA2*

To further analyze the effects of OsSEC24 on the PM sorting of OsPMA2 in rice, we utilized transient expression in rice protoplast isolated from suspension culture cells. ER Tracker™ Blue-White (ER-Tracker™ B-W) is a cell-permeable dye that selectively labels the ER [35]. After Blue White staining, the colocalization of OsSEC24-GFP with Blue-White dye indicated that cytosolic OsSEC24 was recruited to ER for the transport of vesicles budding from ER (Fig. 8A, top, arrowhead). And the colocalization of OsPMA2-mCherry with Blue-White dye showed that OsPMA2 was synthesized in the ER before sorted to the PM (Fig. 8A, bottom). Visual inspection data under confocal microscope that OsPMA2-mCherry was colocalized with OsSEC24-GFP in the cytoplasm suggested that OsPMA2 protein was packaged into OsSEC24 vesicles (about 20–23 h) (Fig. 8B, top). Eventually, the specific OsPMA2 signal was found near the PM, but OsSEC24 was disassembled (about 23–25 h) (Fig. 8B, bottom). Measurements of H^+ flux rates, the real-time kinetics, and of the mean rate of H^+ flux showed that the net H^+ efflux in the *OsPMA2-mCherry*- and *OsSEC24-GFP* double-transgenic rice protoplast was enhanced, compared to *OsPMA2-mCherry* transgenic cells and *mCherry* plus *GFP* double-transgenic cells (Fig. 8C and D). These data indicate that OsPMA2 out

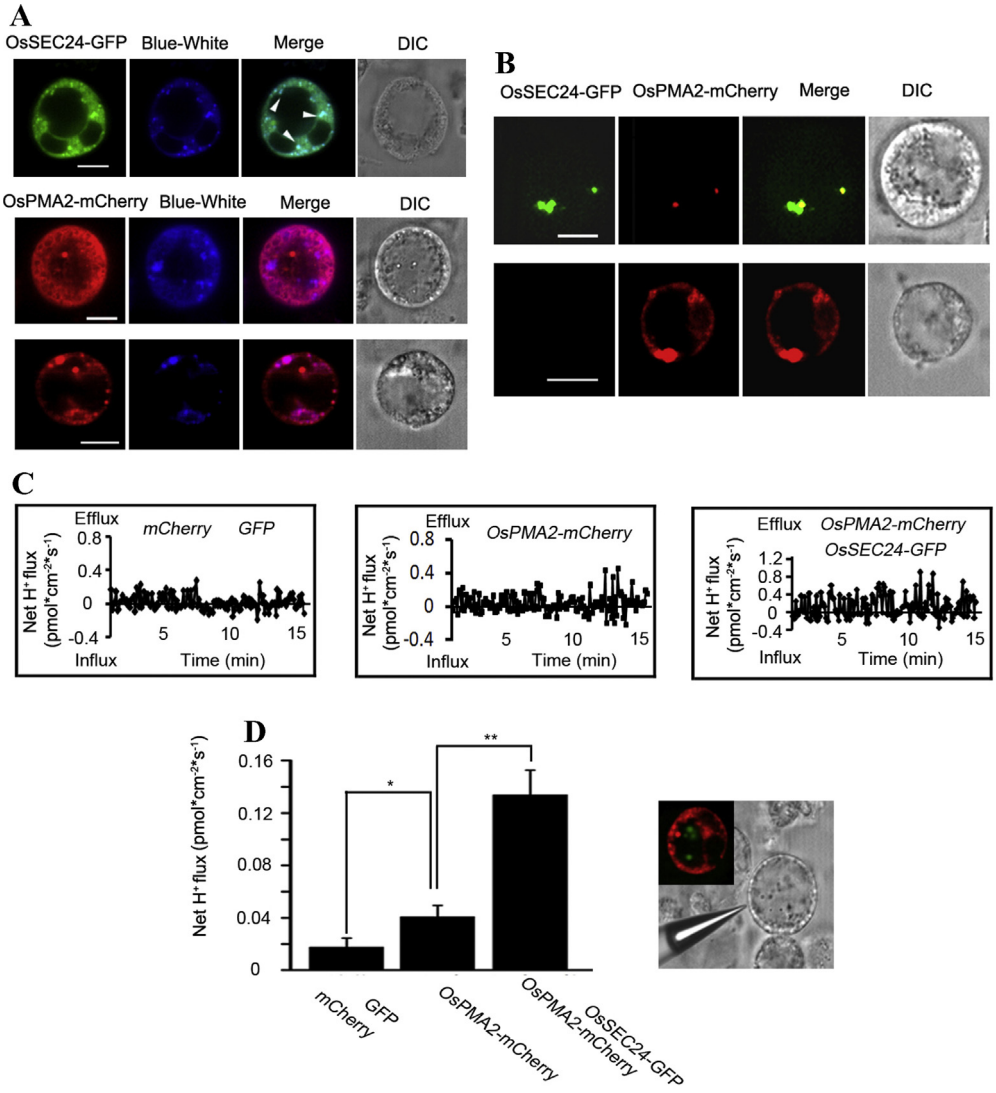

Fig. 8. The effects of OsSEC24 on the transport of OsPMA2 in a rice protoplast. (A) Observation of localization of OsSEC24-GFP (top) and OsPMA2-mCherry (bottom) in transgenic rice protoplast using confocal microscopy after ER-Tracker Blue-White staining. DIC, Differential Interference Contrast. (B) The dynamic localization changes of OsPMA2 and OsSEC24 in *OsPMA2-mCherry* and *OsSEC24-GFP* double-transgenic rice protoplasts from 20 h to 23 h (top) and from 23 h to 25 h (bottom). DIC, differential interference contrast. (C) Kinetics of H^+ flux in *mCherry* plus *GFP* double-transgenic rice protoplasts, *OsPMA2-mCherry* single-transgenic protoplasts and *OsPMA2-mCherry* plus *OsSEC24-GFP* double-transgenic protoplasts. The experiment was performed three times. Results from a representative experiment are shown. (D) The mean rates of H^+ flux in (C), using the mean value of three independent measurements (mean ± SE). Every independent measurement contained >150 replicates. The image shows the measuring position. $^*p < 0.05$ in Student's *t*-test; $^{**}p < 0.01$ in Student's *t*-test. Scale bars for the panels are 10 μm.

of ER is coated by OsSec24 for vesicle transport and that OsSec24 expression in rice protoplast enhances the H^+ extrusion mediated by OsPMA2.

4. Discussion

In this work, we characterized a functional SEC24-like protein in rice (*O. sativa L. cv. Japonica*); we designated this protein as OsSEC24 according to functional complementation experiments in yeast (Fig. 1). OsSEC24 confers tolerance to high-pH and iron-deficiency conditions by enhancing H^+ secretion (Figs. 2, 4 and 5). According to acid growth theory, H^+ excretion increases, resulting in increased activation of cell wall-localized enzymes and elongation growth of plant cells [9,10]. This can explain why *OsSEC24*-transgenic tobacco plants have greater numbers of and longer roots than the wild type controls in plant growth under the conditions of iron deficiency and high pH (Fig. 3A, −Fe, pH 8.0). The utilization of vanadate shows that H^+ secretion promoted by OsSEC24 is attributable to PM H^+-ATPase (Figs. 4 and 5). In rice roots, OsPMA2 is used as the representative of −Fe-responsive H^+-ATPase isoforms (Fig. 6). SEC24 coat protein of COPII vesicles is required for PM sorting of OsPMA2 and OsSEC24 functionally complement SEC24 in yeast (Fig. 7A). And we also show that OsPMA2 is recruited into OsSEC24 vesicles after export from the ER (Fig. 8A and B). Furthermore, H^+ flux measurement in both transgenic yeast and rice protoplasts indicates that OsSEC24 expression increases the H^+ secretion mediated by OsPMA2 (Figs. 7B and C, 8C and D). OsSEC24 seems to play a major role in nutrient acquisition and plant growth by increasing H^+ secretion mediated by H^+-ATPase. However, how OsSEC24 participates in the assembly of coat proteins of COPII vesicle has yet to be elucidated and needs to be further investigated deeply.

In contrast to the Strategy II iron uptake system of grasses, the Strategy I-type of iron absorption is severely affected by high external pH, being restricted because of reduced PM H^+-ATPase activity [32]. The fact indicates that the expression of PM H^+-ATPase isogenes is down-regulated when the external pH increases; this phenomenon has been proven by accumulating evidence in *Arabidopsis* and rice [11,36]. In our study, however, OsSEC24 confers tolerance to high-pH by enhancing H^+ secretion. And *OsSEC24*-transgenic Strategy I-type tobacco displays better growth at high pH than do the wild type, which not only supports acid growth theory but also points to an important function of OsSEC24 in the high pH resistance.

As shown in Strategy I plant's roots, the increase in the PM H^+-ATPase activity with a consequent acidification of the rhizosphere under −Fe is not only due to the growing number of root tips in the plants under −Fe but also to an increased enzyme concentration in each tip notwithstanding other regulatory mechanisms [37]. In the present study, we find that −Fe induces growth of more roots in the *OsSEC24*-transgenic tobacco than wild type (at pH 8.0). And the *OsSEC24*-transgenic tobacco and rice plants have stronger H^+ secretion mediated by PM H^+-ATPase than do the wild type plants under −Fe. Thus, these data suggest that the increased activity of H^+-ATPase under −Fe is not only due to the enhanced root tips and enzyme synthesis but also due to the enhanced OsSEC24 vesicle trafficking at the cellular level.

The PM H^+-ATPase, as a universal electrogenic H^+ pump, is capable of establishing an H^+ electrochemical gradient [38]. The H^+-ATPase-mediated transport participates in the majority of physiological processes, such as acquisition of mineral nutrients by roots, translocation of metabolites, maintenance of cytoplasmic pH, and cell turgor-related functions [39–42]. H^+-ATPase activity is thought to be important for many characteristics of plant growth and development. For example, other studies have shown changes in pump activity in response to a variety of environmental conditions, including salt stress, lighting changes, and pathogens [43]. Moreover, transport of nutrients such as Fe, P, and N is intimately linked to the activity of H^+-ATPases in plants [11,12,34,44,45]. In Strategy I plants, an iron deficiency-responsive PM H^+-ATPase gene in the roots of cucumber is *CsHA1* [45]. The two PM H^+-ATPase genes, *AHA2* and *AHA7*, are involved in the iron deficiency response of *Arabidopsis* roots [36]. In the present work, both OsPMA1 and OsPMA2 transcripts are presented to be markedly upregulated in iron deficient rice roots, and we choose *OsPMA2* as a representative of −Fe-responsive H^+-ATPases in rice root. Here, we show that SEC24 coat protein is a key contributor to the PM sorting of OsPMA2 and OsSEC24 is able to functionally replace SEC24 in yeast. Previously, Shimoni et al. [46] showed in yeast that COPII vesicles are responsible for the transport of Pma1 – which comprises up to 50% of the PM protein of yeast – from ER to Golgi.

The secondary structure prediction in ExPASy HMMTOP database (http://www.expasy.org/) indicates that the typical SEC24 in yeast does not contain a transmembrane domain, and with N-terminus out of the ER lumen (Fig. S2A). In yeast and mammalian cells, the coat protein SEC24 directly recognizes transmembrane proteins by sorting signals on the proteins, but soluble cargoes would require membrane adaptors for SEC24 recognization [46]. However, AtSEC24A (At3g07100), a unique SEC24 homolog in *A. thaliana* SEC24 family, possesses a transmembrane helices with N-terminus in the ER lumen [31] (Fig. S2A). A similar conclusion also holds true for OsSEC24 (Fig. S2A and B). The bioinformatics analysis suggests that AtSEC24A or OsSEC24 might interact with cargoes with a different biochemical mechanism, as compared with SEC24 in yeast and mammalian.

In addition to the standard and essential COPII genes, several homologues of SEC24 have been discovered in genetic screens and database searches. Two SEC24 homologues, which are not important for viability of yeast, at least four mammalian SEC24 isoforms, and three SEC24 family members in *A. thaliana* are known [31,47,48]. However, in rice, little is known about SEC24 in relation to COPII coat proteins, and to our knowledge, this is the first report on this topic.

Acknowledgements

We are grateful to Prof. Yong Hu for providing bioinformatics conduction to the paper. This work was supported by the National Natural Science foundation of China (Grant No: 30971856), Local special project supported by central government-Characteristic key subject Botany and the 7th Beijing Municipal Outstanding Teacher Award. This paper has been edited by professional editors at Editage™, a division of Cactus Communications.

Appendix A. Supplementary data

Supplementary data associated with this article can be found, in the online version, at http://dx.doi.org/10.1016/j.plantsci.2015.01.001.

References

[1] G. Vert, N. Grotz, F. Dédaldéchamp, F. Gaymard, M.L. Guerinot, J.F. Briat, C. Curie, IRT1, an *Arabidopsis* transporter essential for iron uptake from the soil and for plant growth, Plant Cell 14 (2002) 1223–1233.
[2] V. Romheld, H. Marschner, Evidence for a specific uptake system for iron phytosiderophore in roots of grasses, Plant Physiol. 80 (1986) 175–180.
[3] L. Wang, Y.G. Ying, R. Narsai, L.X. Ye, L.Q. Zheng, J.L. Tian, J. Whelan, H.X. Shou, Identification of OsbHLH133 as a regulator of iron distribution between roots and shoots in *Oryza sativa*, Plant Cell Environ. 36 (2013) 224–236.
[4] J.I. Schroeder, E. Delhaize, W.B. Frommer, M.L. Guerinot, M.J. Harrison, L. Herrera-Estrella, T. Horie, L.V. Kochian, R. Munns, N.K. Nishizawa, Y.F. Tsay, D.

Sanders, Using membrane transporters to improve crops for sustainable food production, Nature 497 (2013) 60–66.
[5] Y. Ishimaru, M. Suzuki, T. Tsukamoto, K. Suzuki, M. Nakazono, T. Kobayashi, Y. Wada, S. Watanabe, S. Matsuhashi, M. Takahashi, H. Nakanishi, S. Mori, N.K. Nishizawa, Rice plants take up iron as an Fe^{3+}-phytosiderophore and as Fe^{2+}, Plant J. 45 (2006) 335–346.
[6] N. Bughio, H. Yamaguchi, N.K. Nishizawa, H. Nakanishi, S. Mori, Cloning an iron-regulated metal transporter from rice, J. Exp. Bot. 53 (2002) 1677–1682.
[7] G. Duby, M. Boutry, The plant plasma membrane ATPase: a highly regulated P-type ATPase with multiple physiological roles, Pflugers Arch. 457 (2009) 645–655.
[8] T. Zhao, H.Q. Ling, Effects of pH and nitrogen forms on expression profiles of genes involved in iron homeostasis in tomato, Plant Cell Environ. 30 (2007) 518–527.
[9] D.L. Rayle, R. Cleland, Enhancement of wall loosening and elongation by acid solutions, Plant Physiol. 46 (1970) 250–253.
[10] K.L. Farquharson, SAUR19 links auxin and plasma membrane H^+-ATPases in cell expansion, Plant Cell 26 (2014), http://dx.doi.org/10.1105/tpc.114.127886.
[11] Y.Y. Zhu, T.J. Di, G.H. XU, X. Chen, H.Q. Zeng, F. Yan, Q.R. Shen, Adaptation of plasma membrane H^+-ATPase of rice roots to low pH as related to ammonium nutrition, Plant Cell Environ. 32 (2009) 1428–1440.
[12] M.V.L. Sperandio, L.A. Santos, C.A. Bucher, M.S. Fernandes, S.R. de Souza, Isoforms of plasma membrane H^+-ATPase in rice root and shoot are differentially induced by starvation and resupply of NO_3^- or NH_4^+, Plant Sci. 180 (2011) 251–258.
[13] N. Pietrosemoli, R. Pancsa, P. Tompa, Structural disorder provides increased adaptability for vesicle trafficking pathways, PLoS Comput. Biol. 9 (2013), http://dx.doi.org/10.1371/journal.pcbi.1003144.
[14] C.J. Smith, B.M.F. Pearse, Clathrin: anatomy of a coat protein, Trends Cell Biol. 9 (1999) 335–338.
[15] A. Eugster, G. Frigerio, M. Dale, R. Duden, The alpha-and beta′-COP WD40 domains mediate cargo-selective interactions with distinct di-lysine motifs, Mol. Biol. Cell 15 (2004) 1011–1023.
[16] G. Yang, F. Ma, Y. Wang, C.G. Feng, P. Li, Y. Xu, W.Z. Zhao, L.P. Yin, Vesicle-related OsSEC27P enhances H^+ secretion in the iron deficient transgenic tobacco root, Chin. Sci. Bull. 55 (2010) 3298–3304.
[17] D. Jensen, R. Schekman, COPII-mediated vesicle formation at a glance, J. Cell. Sci. 124 (2011) 1–4.
[18] M. Bagnat, A. Chang, K. Simons, Plasma membrane proton ATPase Pma1p requires raft association for surface delivery in yeast, Mol. Biol. Cell 12 (2001) 4129–4138.
[19] Y. Yamaguchi-Iwai, R. Stearman, A. Dancis, R.D. Klausner, Iron-regulated DNA binding by the AFT1 protein controls the iron regulon in yeast, EMBO J. 15 (1996) 3377–3384.
[20] M.J. Han, K.H. Jung, G. Yi, D.Y. Lee, G. An, Rice Immature Pollen 1 (RIP1) is a regulator of late pollen development, Plant Cell Physiol. 47 (2006) 1457–1472.
[21] S. Tan, R. Han, P. Li, G. Yang, S. Li, P. Zhang, W.B. Wang, W.Z. Zhao, L.P. Yin, Overexpression of the MxIRT1 gene increases iron and zinc content in rice seeds, Transgenic Res. (2014), http://dx.doi.org/10.1007/s11248-014-9822-z.
[22] P. Zhang, S. Tan, J.O. Berry, P. Li, N. Ren, S. Li, G. Yang, W.B. Wang, X.T. Qi, L.P. Yin, An uncleaved signal peptide directs the *Malus xiaojinensis* iron transporter protein Mx IRT1 into the ER for the PM secretory pathway, Int. J. Mol. Sci. 15 (2014) 20413–20433.
[23] Naren, P. Zhang, D.K. Ma, Y. Wang, S. Li, L.P. Yin, Overexpression of OsDPR, a novel rice gene highly expressed under iron deficiency, suppresses plant growth, Sci. China Life Sci. 55 (2012) 1082–1091.
[24] L.P. Yin, T. Sun, W. Li, Transcripts and proteome analysis and membrane vesicle trafficking in rice roots under Fe-deficient condition, Prog. Nat. Sci. 14 (2004) 522–527.
[25] D. Dembéléand, P. Kastner, Fold change rank ordering statistics: a new method for detecting differentially expressed genes, BMC Bioinform. 15 (2014), http://dx.doi.org/10.1186/1471-2105-15-14.
[26] T.A. Patterson, E.K. Lobenhofer, S.B. Fulmer-Smentek, P.J. Collins, T.M. Chu, W.J. Bao, H. Fang, E.S. Kawasaki, J. Hager, I.R. Tikhonova, S.J. Walker, L. Zhang, P. Hurban, F. de Longueville, J.C. Fuscoe, W.D. Tong, L.M. Shi, R.D. Wolfinger, Performance comparison of one-color and two-color platforms within the MicroArray Quality Control (MAQC) project, Nat. Biotechnol. 24 (2006) 1140–1150.
[27] D. Eide, M. Broderius, J. Fett, M.L. Guerinot, A novel iron-regulated metal transporter from plants identified by functional expression in yeast, Proc. Nat. Acad. Sci. U. S. A. 93 (1996) 5624–5628.
[28] P. Li, J.L. Qi, L. Wang, Q.N. Huang, Z.H. Han, L.P. Yin, Functional expression of MxIRT1, from *Malus xiaojinensis*, complements an iron uptake deficient yeast mutant for plasma membrane targeting via membrane vesicles trafficking process, Plant Sci. 171 (2006) 52–59.
[29] L.Y. Wang, B. Feng, P. Li, G. Yang, L.P. Yin, Fusion of MxIRT1 vesicles and plasma membrane is a key regulation step of high affinity iron transport in response to iron supplement in transgenic yeast, Asian J. Chem. 24 (2012) 2394–2400.
[30] X.N. Zhang, Z.H. Han, L.L. Yin, J. Kong, X.F. Xu, X.Z. Zhang, Y. Wang, Heterologous functional analysis of the *Malus xiaojinensis* MxIRT1 gene and the His-box motif by expression in yeast, Mol. Biol. Rep. 40 (2013) 1499–1504.
[31] J.O. De Craene, F. Courte, B. Rinaldi, C. Fitterer, M.C. Herranz, C. Schmitt-Keichinger, C. Ritzenthaler, S. Friant, Study of the plant COPII vesicle coat subunits by functional complementation of yeast *Saccharomyces cerevisiae* mutants, PLOS ONE 9 (2014), http://dx.doi.org/10.1371/journal.pone.0090072.
[32] W. Schmidt, Mechanisms and regulation of reduction-based iron uptake in plants, New Phytol. 141 (1999) 1–26.
[33] G. Rabotti, G. Zocchi, Plasma membrane-bound H^+-ATPase and reductase activities in Fe-deficient cucumber roots, Physiol. Plant 90 (1994) 779–785.
[34] H.Q. Zeng, G. Liu, T. Kinoshita, R. Zhang, Y.Y. Zhu, Q.R. Shen, G.H. Xu, Stimulation of phosphorus uptake by ammonium nutrition involves plasma membrane H^+-ATPase in rice roots, Plant Soil 357 (2012) 205–214.
[35] L. Cole, D. Davies, G.J. Hyde, A.E. Ashford, ER-tracker dye and BODIPY-brefeldin A differentiate the endoplasmic reticulum and golgi bodies from the tubular-vacuole system in living hyphae of *Pisolithus tinctorius*, J. Microsc. 197 (2000) 239–249.
[36] S. Santi, W. Schmidt, Dissecting iron deficiency-induced proton extrusion in *Arabidopsis* roots, New Phytol. 183 (2009) 1072–1084.
[37] M. Dell'Orto, L. Pirovano, J.M. Villalba, J.A. González-Reyes, G. Zocchi, Localization of the plasma membrane H^+-ATPase in Fe-deficient cucumber roots by immunodetection, Plant Soil 241 (2002) 11–17.
[38] M. Palmgren, J. Harper, Pumping with plant P-type ATPases, J. Exp. Bot. 50 (1999) 883–893.
[39] M. Oufattole, M. Arango, M. Boutry, Identification and expression of three new *Nicotiana plumbaginifolia* genes which encode isoforms of a plasma-membrane H(+)-ATPase, and one of which is induced by mechanical stress, Planta 210 (2000) 715–722.
[40] M. Arango, F. Geváudant, M. Oufattole, M. Boutry, The plasma membrane proton pump ATPase: the significance of gene subfamilies, Planta 216 (2003) 355–365.
[41] T.E. Sondergaard, A. Schulz, M.G. Palmgren, Energization of transport processes in plants. Roles of the plasma membrane H^+-ATPase, Plant Physiol. 136 (2004) 2475–2482.
[42] I.R. Baxter, J.C. Young, G. Armstrong, N. Foster, N. Bogenschutz, T. Cordova, W.A. Peer, S.P. Hazen, A.S. Murphy, J.F. Harper, A plasma membrane H^+-ATPase is required for the formation of proanthocyanidins in the seed coat endothelium of *Arabidopsis thaliana*, Proc. Natl. Acad. Sci. 102 (2005) 2649–2654.
[43] V. Vitart, I. Baxter, P. Doerner, J.F. Harper, Evidence for a role in growth and salt resistance of a plasma membrane H^+-ATPase in the root endodermis, Plant J. 27 (2001) 191–201.
[44] C.R. Chang, Y.B. Hu, S.B. Sun, Y.Y. Zhu, G.J. Ma, G.H. Xu, Proton pump OsA8 is linked to phosphorus uptake and translocation in rice, J. Exp. Bot. 60 (2009) 557–565.
[45] S. Santi, S. Cesco, Z. Varanini, R. Pinton, Two plasma membrane H^+-ATPases genes are differentially expressed in iron-deficient cucumber plants, Plant Physiol. Biochem. 43 (2005) 287–292.
[46] Y. Shimoni, T. Kurihara, M. Ravazzola, M. Amherdt, L. Orci, R. Schekman, Lst1p and Sec24p cooperate in sorting of the plasma membrane ATPase into COPII vesicles in *Saccharomyces cerevisiae*, J. Cell Biol. 151 (2000) 973–984.
[47] A. Pagano, F. Letourneur, D. Garcia-Estefania, J.L. Carpentier, L. Orci, J.P. Paccaud, Sec24 proteins and sorting at the endoplasmic reticulum, J. Biol. Chem. 274 (1999) 7833–7840.
[48] K. Tani, Y. Oyama, K. Hatsuzawa, M. Tagaya, Hypothetical protein KIAA0079 is a mammalian homologue of yeast Sec24p, FEBS Lett. 447 (1999) 247–250.